Multistrange Particle Production and the Statistical Hadronization Model

Michal Petráň and Johann Rafelski
Department of Physics, University of Arizona, Tucson, Arizona 85721
(Dated: December 9, 2009)

We consider the chemical freeze-out of Ξ, $\overline{\Xi}$ and ϕ multistrange hadrons within a Statistical Hadronization Model inspired approach. We study particle yields across a wide range of reaction energy and centrality from NA49 at SPS and STAR at RHIC experiments. We constrain the physical conditions present in the fireball source of strange hadrons, and anticipate results expected at LHC.

PACS numbers: 24.10.Pa, 12.38.Mh, 25.75.-q, 13.60.Rj

Introduction: We study multistrange hadron production in the context of the quark-gluon plasma (QGP) formation in relativistic heavy ion collisions [1]. Given the relatively small reaction cross sections of multistrange hadrons in hadron matter, the observed yields of $\Xi(qss)$, $\overline{\Xi}$, $\Omega(sss)$, $\overline{\Omega}$, $\phi(s\bar{s})$ [2–7] are considered probes of the earliest stage of the QGP-fireball hadronization.

The yields of these particles have been considered previously within a global approach, see e.g. [8]. Here we show that it is possible to analyze multistrange hadron yields alone. When this is done we find that multistrange and non-strange hadrons share the same freeze-out condition. We will discuss the meaning of this discovery below addressing dynamics of hadronization. We also address the forthcoming LHC effort to measure multistrange hadron yields in high multiplicity *pp* [9], and soon after, in A+A reactions.

QGP hadronic particle production yields are usually considered within the statistical hadronization model (SHM) [10–12]. SHM has been successful in describing (strange) hadron production in heavy ion collisions for different colliding systems and energies. These results showing successful global fits of particle yields in the SHM framework inspired us to study multistrange hadron yields alone in this separate analysis for the purpose of: i) establishing that SHM is appropriate for describing yields of these particles, ii) assessing if their yields are consistent with the established bulk matter properties of the QGP fireball, thus testing the single freeze-out hypothesis for particles with large and small hadron reaction cross sections, and iii) understanding better how the future LHC results may help arrive at a distinction between SHM model approaches.

SHM Models: We begin by introducing the three principal SHM approaches:

a) Taking the view that SHM has a limited theoretical foundation, one can seek *simplicity* in an effort to obtain a qualitative description of the yields for all hadrons with just a small number of parameters. An additional attraction is that this assumption leads to a model with chemical equilibrium hadron yields is explored. The main result of this approach is that the hadronization in high energy heavy ion collisions at RHIC requires $T \geq 175\,\mathrm{MeV}$, and this high value is close to the lattice crossover temperature, between deconfined and hadron phase [13, 14].

b) In order to arrive at a precise description of the bulk properties, such as strangeness and entropy content of the hadron fireball, we need precise capability to extrapolate hadron yields to unobserved kinematic domains and particle types. This is achieved by introducing statistical occupancy parameters $\gamma_i > 1, i = q, s$. Within this approach there is good systematic behavior of physical observables as a function of collision conditions such as energy or centrality [8, 15–19]. The yields of hadrons are in general found not to be in chemical equilibrium, $\gamma_i \neq 1$; the hadronization temperature is found near to $T \simeq 140$ MeV.

While this value of T could be further away from the deconfinement crossover domain, this is where chiral symmetry restoration is achieved [13, 20], and QGP is transformed into hadrons. Moreover, in this approach the variation of the freeze-out temperature with baryochemical potential parallels the slope seen in the lattice data. Another important outcome of this approach is that a fit to data offers a good statistical significance. Results obtained can be interpreted in terms of a dynamical picture of nearly chemically equilibrated QGP, decaying into free streaming hadrons. The high intrinsic QGP entropy content explains why equilibrated QGP turns into chemically overpopulated (over-saturated) HG phase space – the fast breakup of QGP means that the emerging hadrons do not have opportunity to re-establish chemical equilibrium in the HG phase.

c) *Single Freeze-out* or/and *Strangeness Nonequilibrium* model has as the main objective statistically significant description of hadron yields achieved with minimal effort. Only strangeness chemical non-equilibrium is allowed. This is often enough to produce a decent data fit and to assure that all particles can be formed at the same physical condition [21–25]. The main result of this approach is a hadronization temperature near $T \simeq 160\,\mathrm{MeV}$ which agrees with Hagedorn temperature [26, 27].

Particle ratios of interest: We must include in our theoretical consideration of multistrange hadron yields the contributing yield of decaying hadron resonances. Within SHM these individual yields generally depend on several parameters. The phase space occupancy γ_q scales particle yields according to light quark content, and a similar parameter γ_s refers to strange quark content. Temperature T quantifies the size of accessible phase space. Baryo-chemical potential μ_B differentiates baryons from antibaryons and strange chemical potential

$\mu_{\rm S}$ does the same for strangeness. There is also a potential $\mu_{\rm I3}$ related to different number of up and down quarks which is constrained by proton and neutron asymmetry in colliding nuclei, and the overall yield is normalized by a volume parameter V.

By considering the ratio

$$\frac{\Xi}{\phi} \equiv \sqrt{\frac{\overline{\Xi}^+\Xi^-}{\phi\phi}} \simeq \gamma_q f(T), \qquad (1)$$

we eliminate in good approximation most of the SHM parameter dependencies since:

i) By taking the product of particle and antiparticle, we eliminate baryo-chemical potential $\mu_{\rm B}$ as well as strange chemical potential $\mu_{\rm S}$.

ii) We also eliminate the strange quark phase space occupancy γ_s, because the strange and anti-strange quark content in the numerator and denominator is the same.

iii) The overall normalization is eliminated by the fact that we have the same number of hadrons in the ratio numerator and denominator.

The Ξ/ϕ ratio depends on the probability of finding a non-strange $d,\bar{d}$-quark at the formation of $\Xi^-(dss)$ and $\overline{\Xi}^+(\bar{d}\bar{s}\bar{s})$, respectively. This is expressed by the light quark phase space occupancy γ_q. Furthermore, temperature T controls the magnitude of

$$f(T) \simeq \sum_i \frac{g_i}{3}\left(\frac{m_{\Xi_i}}{m_\phi}\right)^{3/2} e^{\frac{m_\phi - m_{\Xi_i}}{T}} \qquad (2)$$

the (non-relativistic) phase space ratio of Ξ^- and ϕ. $\Xi(1321)$ is always a decay product of $\Xi^*(1530)$. Thus aside of the ground state $i = 1 : \Xi(1321)$, $g_1 = 2$ one must include in the sum the $\Xi^*(1530)$, $g_2 = 4$ resonance. Consideration of this special yield ratio parallels the earlier effort made to identify γ_s/γ_q in Ref.[28].

We extend our considerations to include single strange $\mathrm{K}^+(u\bar{s}), \mathrm{K}^-(\bar{u}s)$ mesons and triple strange $\Omega^-(sss), \overline{\Omega}^+(\bar{s}\bar{s}\bar{s})$ baryons considering the ratios:

$$\frac{\Xi}{\mathrm{K}} \equiv \sqrt{\frac{\overline{\Xi}^+\Xi^-}{\mathrm{K}^+\mathrm{K}^-}} = \gamma_s f_1(T); \quad \frac{\Omega}{\phi} = \sqrt{\frac{\overline{\Omega}^+\Omega^-}{\phi\phi}} = \gamma_s f_2(T). \quad (3)$$

Given the quark content, both Ξ/K and Ω/ϕ are proportional to strange quark yield, i.e. the strange quark phase space occupancy γ_s and a function $f_i(T)$.

The arguments leading to Eq. (1), Eq. (3) are strictly valid only in Boltzmann approximation. Considering quantum statistics, there is some residual dependence of $f(T)$ on chemical parameters, involving higher powers of γ_q for the ratio Ξ/ϕ Eq. (1), and higher powers of γ_s for the ratio Ξ/K Eq. (3). In order to estimate the magnitude of the quantum statistics effect we calculate the actual particle ratios with SHAREv2 [11] using both quantum and Boltzmann statistics. We find that the Boltzmann approximation we used overestimates Ξ/ϕ by 0.25%, which is always negligible. For Ξ/K, we find that it is overestimated by Boltzmann approximation by up to 4%, the relatively larger effect is due to the relatively low mass of the kaon. Since the experimental error is much greater we continue to consider the simple theoretical Boltzmann yields. When further below we consider ratios involving pions, all results are obtained using SHAREv2, which accounts for resonance decays and all yields can be obtained using quantum statistics.

TABLE I: Fit parameters used to determine particle yields for incompatible centrality bins using $f(N_{\rm part}) \equiv a \cdot N_{\rm part}^b + c$ (see text for details).

	a	b	c
π^-	4.179×10^{-1}	1.072	7.107×10^{-1}
π^+	4.247×10^{-1}	1.048	6.422×10^{-1}
K^+	5.433×10^{-2}	1.111	-1.014×10^{-1}
K^-	4.812×10^{-2}	1.107	-3.859×10^{-2}
Ξ^-	1.228×10^{-3}	1.247	-4.678×10^{-3}
$\overline{\Xi}^+$	8.978×10^{-4}	1.221	9.390×10^{-4}
ϕ^0	4.162×10^{-3}	1.203	-9.311×10^{-3}

Experimental data: We consider 4π data from the CERN-SPS NA49 experiment, and for the STAR experiment at RHIC the acceptance rapidity interval is $|y| < 0.5$; therefore at RHIC we use the yield per unit of rapidity dN/dy and omit the differential dy when referring to relative yields. For the ϕ meson we consider the recently published data from STAR [2] and the updated data from NA49 [3]. We collected the necessary data for Ξ and $\overline{\Xi}$ baryons from Refs. [4–6].

We do not use NA49 158 GeV results, since these experimental results do not allow to interpolate the different centrality bins used to measure different multistrange particle yields. We could not simply combine data from different centrality bins seen the variation of yields with centrality (that is γ_s). The STAR 62 experiment provides data in several centrality bins, defined as a percentage of the most central collisions: data from the most central collisions is found in the centrality $0-5\%$ interval and the most peripheral collision results presented are in $70-80\%$ bin. The relation to $N_{\rm part}$ and/or impact parameter b is discussed in [7].

We use recent data for $\mathrm{K}^\pm$ mesons from STAR experiments at both $\sqrt{s_{NN}} = 200$ and 62.4 GeV from [7]. For the SPS NA49 data we use yields from [29, 30].

We note that different centrality bins are often chosen for different particle types. In order to be able to form particle ratios in a common centrality interval, we inter/extrapolate, that is fit individual yields as a function of the number of participants using a simple functional form $f(N_{\rm part}) \equiv a \cdot N_{\rm part}^b + c$. We show the fit parameters a,b and c in Table I and compare the experimental results and the fit in figure 1.

Particle ratios: After this preparation we can form ratios of particle yields as shown in figure 2 and table II. We note that the Ξ/ϕ relative yield does not change much over a wide range of energies and centralities, in contrast to the individual hadron yields which enter the

TABLE II: Values of ratios Ξ/ϕ Eq. (1), Ξ/K Eq. (3), Ξ/π and ϕ/π Eq. (4) obtained from the data and the resulting estimated uncertainty in γ_s and γ_q, respectively. When symbol 'E' is shown in the error column, the data ratio is result of interpolation and/or extrapolation needed to account for different centrality bins.

Experiment	Centrality	$\Xi/\phi \times 10$	$\delta\gamma_q$	$\Xi/\mathrm{K} \times 10^2$	$\delta\gamma_s$	$\Xi/\pi \times 10^3$	$\phi/\mathrm{K} \times 10$	$\phi/\pi \times 10^2$
STAR 62	0-5%	3.04	E	4.19	9.6%	6.22	1.38	2.04
STAR 62	5-10%	3.00	E	4.08	9.2%	6.20	1.36	2.06
STAR 62	10-20%	2.94	E	4.06	9.3%	5.98	1.38	2.04
STAR 62	20-40%	2.88	12.5%	3.79	E	5.48	1.32	1.91
STAR 62	40-60%	2.85	14.6%	3.38	E	4.65	1.18	1.63
STAR 62	60-80%	2.49	19.3%	2.84	E	3.45	1.14	1.38
STAR 200	0-20%	3.02	11.8%	4.06	12.9%	6.04	1.34	$^a 2.54^{+0.21}_{-0.09}$
SPS 80 AGeV	7%	3.33	24.5%	3.04	22.7%	2.60	0.83	0.88
SPS 40 AGeV	7%	2.45	42.1%	1.89	18.0%	3.23	0.78	0.83
SPS 30 AGeV	7%	2.57	66.5%	1.85	24.3%	2.10	0.63	0.72

[a] For STAR 200 ϕ/π considering figure 14 in [2] we give an average of data for centralities up to 50%.

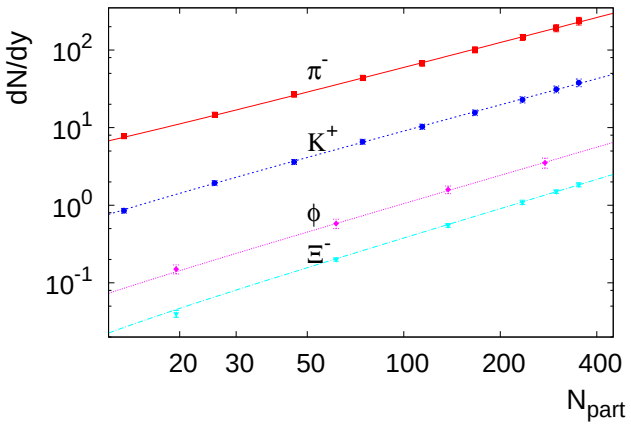

FIG. 1: (Color online) Data points (full symbols) of particle yields used in the analysis, and their respective fitted centrality dependence.

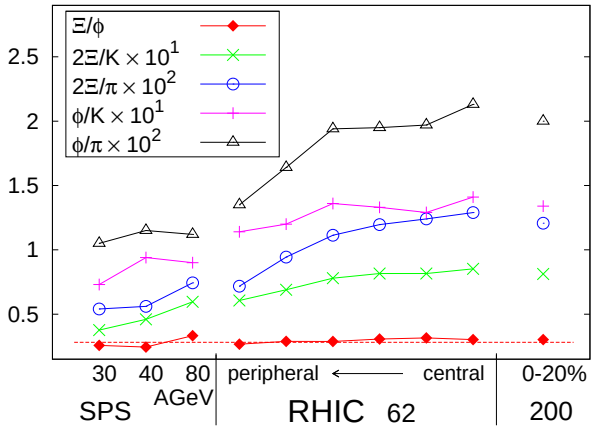

FIG. 2: (Color online) Data points of Ξ/ϕ Eq. (1), Ξ/K Eq. (3), Ξ/π and ϕ/π Eq. (4). The straight line for $\Xi/\phi = 0.281$.

ratio. The average value of all available data points is $\Xi/\phi = 0.281$ with an error at 15% level.

The remarkable result, the constancy of Ξ/ϕ means that at SPS and RHIC energies the mechanisms and conditions at which double-strange particles are produced are very similar and that, according to Eq. (1), there is a constraint between values of γ_q and T, which we now explore in figure 3 where we show in the T, γ_q plane the theoretical SHM results as lines for a constant ratio Ξ/ϕ. These values are obtained using SHAREv2 and varying γ_q and T, with all other model parameters fixed to a reasonable physical values. In this way we also confirm once again the analytical formula Eq. (2).

We limit the magnitude of γ_q by a critical value of light quark phase space occupancy $\gamma_q^{\rm crit}$. $\gamma_{\pi^0} \equiv \gamma_q^2 \leq (\gamma_q^{\rm crit})^2 = \exp(m_{\pi^0}/T)$, which is the condition where the pion phase space distribution function diverges for $m_{\pi^0} = 135$ MeV/c^2. The experimental values $\Xi/\phi \simeq 0.281 \pm 15\%$ are found consistent with all SHM models in that for $\gamma_q = 1$ we find the value $T = 170 \pm 10$ MeV, and for $\gamma_q \to 1.63$ a value $T \to 140$ MeV.

Test of SHM models: We have seen that hadronization of Ξ and ϕ is consistent with the three different SHM models, but there is an interesting constraint between T, γ_q arising from the constancy of the relative Ξ and ϕ yield. We see also in figure 2 that the variation of Ξ/K is significant, it changes by a factor of 2.3 in the entire data range. Considering that we already have established by the study of Ξ/ϕ that the hadronization temperature does not vary this indicates that there is a variation of γ_s value by a factor of about 2.3 in the data range. We conclude that a fixed value $\gamma_s = 1$ cannot be chosen. This rules out the SHM model **a)**. We also note that this argument can be made in the same way considering the variation of the other ratios in fig. 2, e.g. Ξ/π and ϕ/K.

SHM results for Ξ/K and Ω/ϕ in T, γ_s plane are shown in figure 4, obtained by the same method as before; i.e. using SHARE with other SHM parameters fixed at an appropriate value. For a given Ξ/K and/or Ω/ϕ a slight γ_q dependence remains, since there are unrelated reso-

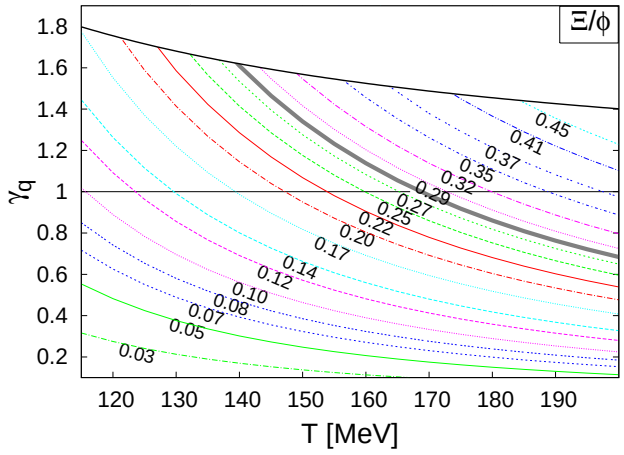

FIG. 3: (Color online) Lines of a constant given ratio Eq. (1) $\Xi/\phi \in [0.03, 0.45]$ in the T, γ_q plane. The lines for $\gamma_q = 1$ and $\gamma_q = \gamma_q^{\rm crit}$ are presented by solid black lines. The average result, 0.281, of all SPS and RHIC experiments is highlighted by a thick gray line. As this ratio is considered constant, this line indicates the prediction of LHC results.

nances decaying into K (and to lesser degree Ξ). Thus we present for each fixed value of Ξ/K two extremes: $\gamma_q = 1$, and $\gamma_q = \gamma_q^{\rm crit}$. The effect is depicted in figure 4a in terms of two lines shown by the same line type.

Note that similarly as for γ_q, there is a critical value for γ_s based on the Bose-Einstein condensation of the η meson ($\eta = 0.55(\mathrm{u\overline{u}} + \mathrm{d\overline{d}}) + 0.45\mathrm{s\overline{s}}$ [31, 32]). The large values of γ_s could be relevant to the future LHC results. To compare theory and experiment we show the thick 0-20% STAR 62 line and by looking at the bottom frame of figure 4 we obtain the prediction: $5.5 \times 10^{-2} < \Omega/\phi < 7.0 \times 10^{-2}$, the variation due to variability of hadronization temperature.

In order to further elaborate the validity of models **b), c)** we show on the right in table II the ratios Ξ/π, ϕ/K, and ϕ/π, where

$$\frac{\Xi}{\pi} \equiv \sqrt{\frac{\Xi^-\overline{\Xi}^+}{\pi^-\pi^+}}; \quad \frac{\phi}{\mathrm{K}} \equiv \sqrt{\frac{\phi\phi}{\mathrm{K^-K^+}}}; \quad \frac{\phi}{\pi} \equiv \sqrt{\frac{\phi\phi}{\pi^-\pi^+}}. \quad (4)$$

The experimental Ξ/π and ϕ/π relative yields vary by a factor $\simeq 3.5$ in both cases. In figure 5 we show the ϕ/π ratio and compare to theory as a function of γ_s at fixed given T. Model **b)** with $T \simeq 140, \gamma_q = \gamma_{\rm crit}$ implies that the different experimental results correspond to $1 < \gamma_s < 2.4$. These values are consistent with the large value of $\gamma_q = \gamma_{\rm crit} \simeq 1.6$. On the other hand, for $\gamma_q = 1$ several fixed T lines nearly coincide in the interesting range $210 \geq T \geq 160$ MeV. This means that the growth in yield of ϕ is nearly compensated by the growth in π-multiplicity. It will be very interesting to see how LHC results will line up in this presentation, since we see that the high energy RHIC results even at $\gamma_q = 1$ imply $\gamma_s > 1$. A value $\gamma_s > 1$ is incompatible with the picture of strangeness production in hadron collisions, and implies the presence of a strangeness dense QGP phase as a source of hadrons.

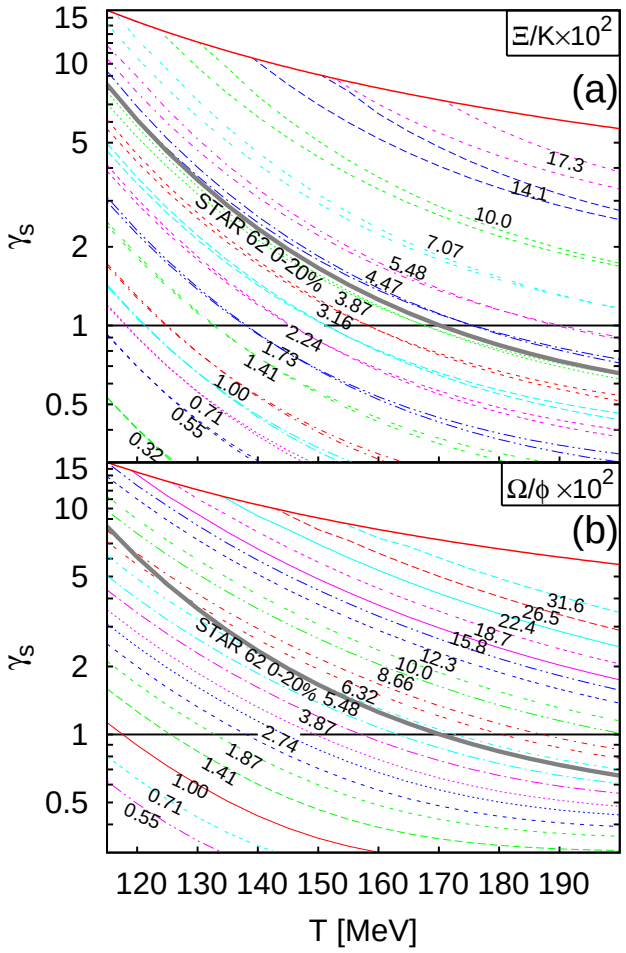

FIG. 4: (Color online) Lines of constant ratio Ξ/K (a) and Ω/ϕ (b). Experimental data from most central 0-20% STAR 62 are indicated by a thick line (b), and is assumed in the bottom frame as a prediction. See text for more detail.

Behavior at LHC: As already remarked the ratio $\Xi/\phi \simeq 0.28$ is firmly constrained and cannot change. Even under the extreme LHC conditions we expect that this ratio will be the same as at RHIC. However, considerable changes can be expected for other (multi)strange particle ratios which were discussed earlier [34, 35]. Here we will mainly address the ϕ/π ratio.

When we accept the premise, that entropy and strangeness are conserved during the hadronization, we can predict values of the phase space occupancy γ_s in chemical semi- and non-equilibrium models for LHC. We expect a 20% increased value of strangeness over entropy $s/S \simeq 0.037$ [35]. For the two models under consideration ($T = 140$ MeV,$\gamma_q = \gamma_q^{critical}$ and 170 MeV,$\gamma_q = 1$) this value suggests [34] $\gamma_s/\gamma_q \simeq 1.55$. The expected ϕ/π ratio is 2.95×10^{-2} and 3.90×10^{-2} for the two models as indicated by the boundaries of the LHC band in figure 5. Experimental results of this magnitude requires $\gamma_s > 1$

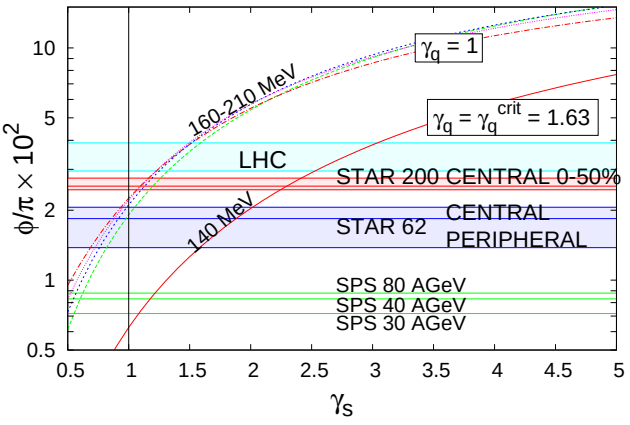

FIG. 5: (Color online) The relative ϕ/π Eq. (4) yield as a function of γ_s in several hadronization scenarios, see text. The vertical solid black line shows the chemical equilibrium with $\gamma_s = 1$. For experimental data see table II. Predicted values for LHC are indicated in blue.

and concludes in favor of chemical non-equilibrium the still ongoing discussion of chemical equilibrium models.

Summary and conclusions: We find that the relative particle yield Ξ/ϕ is practically constant as function of centrality and reaction energy at RHIC and SPS. We find that these particles, despite their small reaction cross-sections are emerging at the same hadronization condition as all bulk particles. This result was anticipated [33] for a fast expanding QGP fireball which under-cools and rapidly breaks apart (hadronizes), and has been used extensively in single hadronization models [16, 18, 19, 22]

Variation in the ratio Ξ/K (and thus also ϕ/K $\propto \gamma_s/\gamma_q$) implies a variation in strange phase space occupancy γ_s, in agreement with the expectation that strangeness production grows with energy and centrality of the collision. This experimental result is incompatible with the chemical equilibrium model **a)**, for which also the parameter γ_s is fixed to 1 by definition.

Considering further the yields Ξ/π and ϕ/π consistency with the bulk matter particle production rates is arrived at within the chemical non-equilibrium model **b)** with $\gamma_q > 1$ and $\gamma_s > 1$. These values imply that the observed strange hadrons yields are above chemical equilibrium, a feature predicted to be signature for hadronization of a QGP-fireball [36]. The expected further increase of $\gamma_s > 1$ at LHC implies a further increase of the ϕ/π ratio, providing a clear distinction between chemical non-equilibrium model **b)** and semi-equilibrium model **c)**.

Our results show that the yields of all multistrange hadrons available today are 1) compatible with the SHM picture of hadron formation, 2) are well described by current chemical nonequilibrium hadronization models in the parameter domain obtained from the other hadron yields, 3) these data are incompatible with the chemical equilibrium single-freeze-out SHM. A critical test of our approach is that in LHC-ion experiments the Ξ/ϕ ratio remains the same as has been observed at SPS and RHIC.

Acknowledgments JR would like to thank Z.L. Matthews and O. Villalobos Baillie of Birmingham University and CERN-ALICE collaboration for interesting discussions. This work was supported by a grant from the U.S. Department of Energy, DE-FG02-04ER41318 .

[1] A.R. Timmins (STAR), Nucl. Phys. **A830**, 829c (2009).
[2] B.I. Abelev (STAR), Phys. Lett. **B673**, 183 (2009).
[3] C. Alt (NA49), Phys. Rev. **C78**, 044907 (2008).
[4] C. Alt (NA49), Phys. Rev. **C78**, 034918 (2008).
[5] J. Adams (STAR), Phys. Rev. Lett. **98**, 062301 (2007).
[6] J. Speltz, Ph.D. thesis (2006), http://drupal.star.bnl.gov/STAR/theses/ph-d/jeff-speltz.
[7] B.I. Abelev (STAR), Phys. Rev. **C79**, 034909 (2009).
[8] I. Kuznetsova, J. Letessier & J. Rafelski, Acta Phys. Polon. **B40**, 1013 (2009).
[9] Z. L. Matthews (ALICE) (2010), *Strangeness in High Multiplicity pp Collisions at ALICE LHC*, presented at SQM09, Buzios, Brazil, in proceedings.
[10] J. Letessier & J. Rafelski, Camb. Monogr. Part. Phys. Nucl. Phys. Cosmol. **18**, 1 (2002).
[11] G. Torrieri et al., Comput. Phys. Commun. **167**, 229 (2005); and **175**, 635 (2006).
[12] F. Becattini & R. Fries, (2009), arXiv 0907.1031.
[13] Z. Fodor & S. D. Katz, (2009), arXiv 0908.3341.
[14] P. Braun-Munzinger & J. Wambach, Rev. Mod. Phys. **81**, 1031 (2009).
[15] G. Torrieri & J. Rafelski, New J. Phys. **3**, 12 (2001).
[16] J. Rafelski, J. Letessier & G. Torrieri, Phys. Rev. **C72**, 024905 (2005).
[17] J. Letessier & J. Rafelski, Phys. Rev. **C73**, 014902 (2006).
[18] J. Letessier & J. Rafelski, Eur. Phys. J. **A35**, 221 (2008).
[19] J. Rafelski & J. Letessier, J. Phys. **G36**, 064017 (2009).
[20] R. Gupta (2009), DPF2009, arXiv 0912.1374.
[21] F. Becattini et al., Phys. Rev. **C64**, 024901 (2001).
[22] W. Broniowski & W. Florkowski, Phys. Rev. **C65**, 064905 (2002).
[23] F. Becattini et al., Phys. Rev. **C69**, 024905 (2004).
[24] F. Becattini, J. Manninen & M. Gazdzicki, Phys. Rev. **C73**, 044905 (2006).
[25] F. Becattini & J. Manninen, J. Phys. **G35**, 104013 (2008).
[26] R. Hagedorn & J. Ranft, Nuovo Cim. Suppl. **6**, 169 (1968).
[27] R. Hagedorn & J. Rafelski, Phys. Lett. **B97**, 136 (1980).
[28] J. Rafelski & J. Letessier, Nucl. Phys. **A715**, 98 (2003).
[29] C. Alt et al. (NA49), Phys. Rev. **C77**, 024903 (2008).
[30] S. V. Afanasiev (NA49), Phys. Rev. **C66**, 054902 (2002).
[31] V. Uvarov, Phys. Lett. **B511**, 136 (2001).
[32] J.-W. Li & D.-S. Du, Phys. Rev. **D78**, 074030 (2008).
[33] J. Rafelski & J. Letessier, Phys. Rev. Lett. **85**, 4695 (2000).
[34] I. Kuznetsova & J. Rafelski, Eur. Phys. J. **C51**, 113 (2007).
[35] J. Letessier & J. Rafelski, Phys. Rev. **C75**, 014905 (2007).
[36] J. Rafelski, Phys. Rep. **88**, 331 (1982).